

# Cascade Catalysis Through Bifunctional Lipase Metal Biohybrids for the Synthesis of Enantioenriched O-Heterocycles from Allenes

Janne M. Naapuri,<sup>[a, b, c]</sup> Noelia Losada-Garcia,<sup>[c]</sup> Robin Alexander Rothemann,<sup>[b]</sup> Manuel Carmona Pichardo,<sup>[b]</sup> Martin H. G. Precht,<sup>[d]</sup> Jose M. Palomo,<sup>\*,[c]</sup> and Jan Deska<sup>\*,[a, b]</sup>

Lipase/metal nanobiohybrids, generated by growth of silver or gold nanoparticles on protein matrixes are used as highly effective dual-activity heterogeneous catalysts for the production of enantiomerically enriched 2,5-dihydrofurans from allenic acetates in a one-pot cascade process combining a lipase-mediated hydrolytic kinetic resolution with a metal-catalyzed allene cycloisomerization. Incorporating a novel strategy based on enzyme-polymer bioconjugates in the nanobiohybrid preparation enables excellent conversions in the process. *Candida antarctica* lipase B (CALB) in combination with a dextran-based

polymer modifier (DexAsp) proved to be most efficient when merged with silver nanoparticles. A range of hybrid materials were produced, combining Ag or Au metals with *Thermomyces lanuginosus* lipase (TLL) or CALB and its DexAsp or polyethyleneimine polymer bioconjugates. The wider applicability of the biohybrids is demonstrated by their use in allenic alcohol cyclizations, where a variety of dihydrofurans are obtained using a CALB/gold nanomaterial. These results underline the potential of the nanobiohybrid catalysis as promising approach to intricate one-pot synthetic strategies.

## Introduction

Cascade reactions, where multiple chemical transformations are incorporated into a single process step, are of great importance for sustainable and economic process development. These kind of one-pot designs reduce avoidable time and resource consumption and waste production by eliminating unnecessary work-up and purification steps.<sup>[1]</sup> Such cascade processes are typical for the field of biocatalysis, where the natural affinity of the various enzymes towards similar reaction conditions and the broad tolerance of functional groups and other biocatalysts facilitates the design of elaborate domino processes.<sup>[2]</sup> Combin-

ing biocatalysis in cascade fashion with metal-catalysis offers a wide variety of attractive options, with prototypical examples including a number of dynamic kinetic resolution strategies.<sup>[3]</sup> However, the approach suffers from troublesome challenges, most notably poisoning effects between metal entities and biomolecules.<sup>[3a-c]</sup> Recent developments in the field of nanotechnology have led to emergence of enzyme-metal nanobiohybrids,<sup>[4]</sup> with potential for acting as bifunctional heterogeneous catalysts.<sup>[5]</sup> Here, the protein acts as a matrix for the formation of metal nanoparticles, resulting in a hybrid material, which retains activities of both the enzyme and metal constituents. Amongst the established applications of the enzyme-metal nanobiohybrids are one-pot processes capitalizing on the dual-activity of the catalytic entity, including hydrolytic/reductive cascade reactions and a dynamic kinetic resolution of amines.<sup>[4b]</sup>


Allenenes have been established as versatile building blocks for synthesis of complex organic structures due to the unique reaction scope offered by the cumulated carbon-carbon double-bonds.<sup>[6]</sup> Particularly, allenic compounds with a nucleophilic functionality have been widely employed for syntheses of heterocyclic entities.<sup>[7]</sup> We recently reported on a chemoenzymatic sequential one-pot design for arylation cyclization of  $\alpha$ -hydroxyallenenes, where a biocatalytic halogenation was paired with palladium catalyzed Suzuki and Sonogashira-type cross couplings.<sup>[8]</sup> As part of the study, an enzyme-metal nanoparticle biohybrid consisting of glucose oxidase from *Aspergillus niger* and palladium nanoparticles (GOx/PdNP) was used as a dual catalyst. Interestingly, the heterogeneous catalyst exhibited potential for the cycloisomerization of allenic alcohols as a side reaction in a process where an enzymatic bromocyclization was the desired outcome (Scheme 1a). The allenol cyclization is well-established in homogeneous catalysis, usually associated


[a] J. M. Naapuri, Prof. Dr. J. Deska  
Department of Chemistry  
University of Helsinki  
A. I. Virtasen aukio 1, 00560 Helsinki (Finland)  
E-mail: jan.deska@helsinki.fi  
Homepage: www.deskalab.com

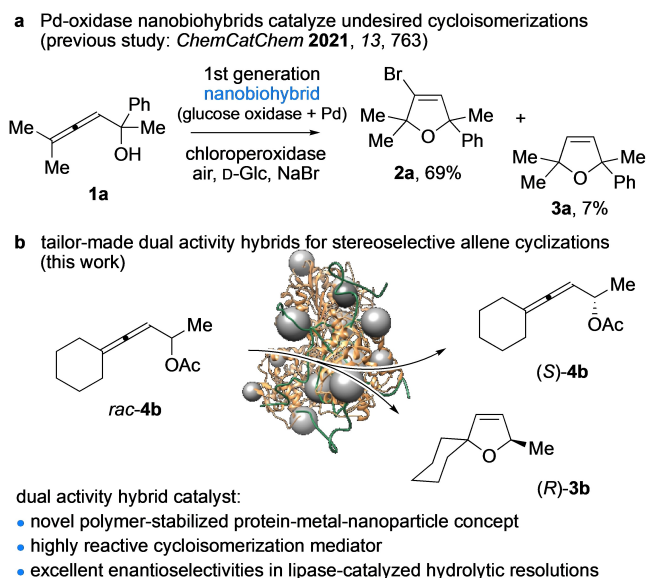
[b] J. M. Naapuri, R. A. Rothemann, M. C. Pichardo, Prof. Dr. J. Deska  
Department of Chemistry  
Aalto University  
Kemistintie 1, 02150 Espoo (Finland)

[c] J. M. Naapuri, Dr. N. Losada-Garcia, Dr. J. M. Palomo  
Instituto de Catalisis y Petroleoquímica (ICP), CSIC  
C/ Marie Curie 2, 28049, Madrid (Spain)  
E-mail: josempalomo@icp.csic.es

[d] Dr. M. H. G. Precht  
Instituto Superior Técnico  
Universidade de Lisboa  
Av. Rovisco Pais 1, 1049-001 Lisboa (Portugal)

 Supporting information for this article is available on the WWW under <https://doi.org/10.1002/cctc.202200362>

 © 2022 The Authors. ChemCatChem published by Wiley-VCH GmbH. This is an open access article under the terms of the Creative Commons Attribution Non-Commercial License, which permits use, distribution and reproduction in any medium, provided the original work is properly cited and is not used for commercial purposes.



**Scheme 1.** Allenol cyclizations: from undesired side reactions to effective tools in stereoselective organic synthesis.

with Au and Ag catalysis,<sup>[7a,9]</sup> although it has been observed in heterogeneous Pd nanoparticle catalysis before.<sup>[10]</sup> The finding inspired us to pursue the 2,5-dihydrofuran-forming process in more detail, and in conjunction with an enzymatic function to explore new cascade applications for the dual-activity nanobiohybrids. Lipases have been in the forefront throughout the emergence of biocatalysis as a powerful tool for synthesis and industry. The broad applicability and tolerance in both hydrolytic and alcoholic processes has seen the enzymes generate extensive interest. Of particular appeal for synthesis are kinetic resolution techniques, taking advantage of the remarkable selectivities offered by the biocatalysts.<sup>[11]</sup> We envisioned that a lipase-induced kinetic resolution hydrolysis of allenic acetates could be combined in a one-pot process with a metal-catalyzed hydroxyallene cyclization, where the enzyme-metal nanoparticle biohybrid would act as a single dual-active entity for heterogeneous catalysis, to synthesize directly optically pure 2,5-dihydrofurans (Scheme 1b). The belief was supported by positive reports from the groups of Krause and Bäckvall in their efforts to produce *O*-heterocycles from allenic compounds via

cascade combinations of lipase kinetic resolution with metal-induced cycloisomerizations under homogeneous conditions.<sup>[12]</sup>

## Results and Discussion

We began our investigation with the preparation a range of metal nanoparticles on different lipase matrixes. *Candida antarctica* lipase B (CALB) was chosen as the prototype enzyme due to its robustness and stability in harsh conditions in addition to it being successfully implemented in nanobiohybrids previously.<sup>[4]</sup> Due to their well-established applicability in cyclizations of allenes, silver and gold were elected as the metals to be included in the biohybrid synthesis, in addition to the benchmark palladium from our previous study. Here, incubating free CALB enzyme in aqueous solutions containing the desired metal salts at room temperature for 24 h produced solid biohybrid materials, recoverable by centrifugation and lyophilization (Figure 1). Combining the lipase with AgNO<sub>3</sub> gave the hybrid CALB/AgNP-1. The accumulated silver nanoparticles comprised 26% (w/w) of the material, as analyzed by ICP-OES (Table 1). TEM and SEM analysis of the CALB/AgNP-1 hybrid revealed a typical mesoporous amorphous aggregated structure, where the silver nanoclusters had formed in the size range of 10 nm (Figure 2). Similarly, gold biohybrid CALB/AuNP-1 was synthesized using HAuCl<sub>4</sub> as metal source. Noticeable differences were observed on the growth of Au nanoparticles on the CALB aggregate compared to the Ag hybrid, as the accumulated metal content was lower at 16% (w/w) (Table 1) and the gold nanocluster size was larger, in the range of 20 nm according to TEM analysis (Figure 2). Growing palladium nanoparticles on the protein matrix using Pd(OAc)<sub>2</sub> salt resulted in

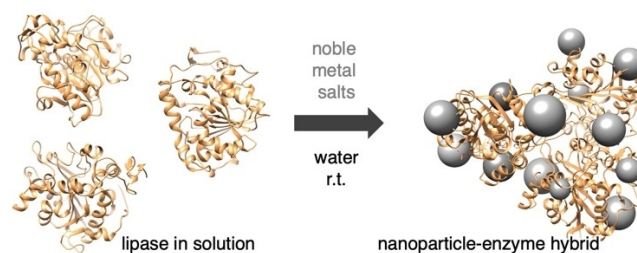


**Figure 1.** Representation of lipase-metal nanobiohybrid synthesis.

**Table 1.** Synthesis of enzyme-metal nanobiohybrids.

Entry	Biohybrid	Metal salt	Additive	Metal content [% (w/w)]
1	CALB/AgNP-1	AgNO <sub>3</sub>	–	26
2	CALB/AgNP-2	AgNO <sub>3</sub>	DexAsp (6 kDa)	21
3	CALB/AgNP-3	AgNO <sub>3</sub>	DexAsp (2 MDa)	26
4	CALB/AgNP-4	AgNO <sub>3</sub>	PEI (0.8 kDa)	24
5	CALB/AgNP-5	AgNO <sub>3</sub>	PEI (750 kDa)	26
6	CALB/AuNP-1	HAuCl <sub>4</sub>	–	16
7	CALB/AuNP-2	HAuCl <sub>4</sub>	DexAsp (6 kDa)	4
8	CALB/PdNP	Pd(OAc) <sub>2</sub>	–	26
9	TLL/AuNP	AgNO <sub>3</sub>	–	33
10	TLL/AgNP	HAuCl <sub>4</sub>	–	33

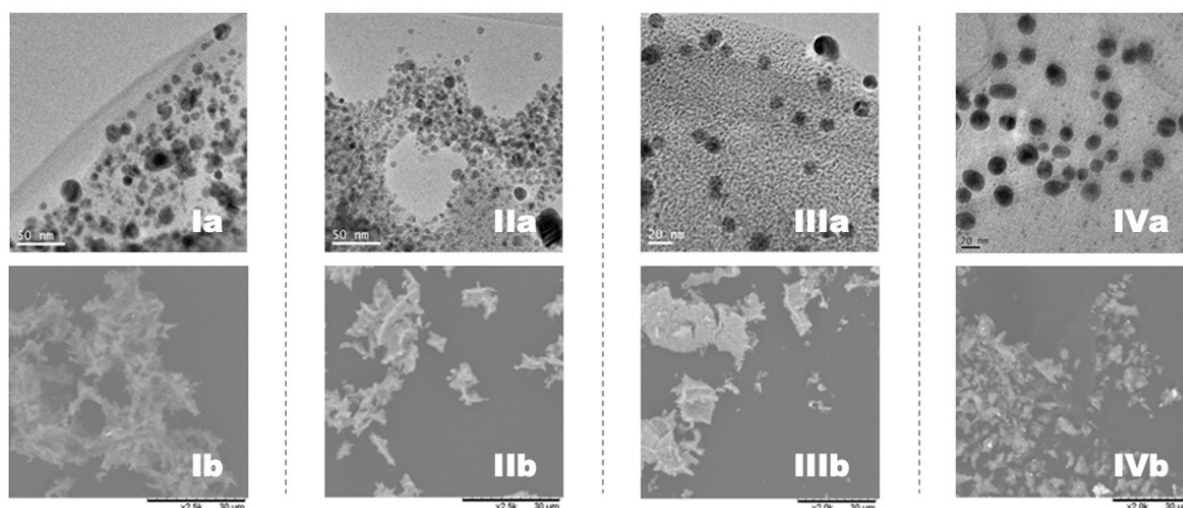


**Figure 2.** Physicochemical characterization of selected nanobiohybrids (a: TEM images, b: SEM images): (I) CALB/AgNP-1, (II) CALB/AgNP-2, (III) CALB/AgNP-3, (IV) CALB/AuNP-1.

the hybrid CALB/PdNP, which exhibited similar metal content as the silver biohybrid with 26% (w/w).

In addition to the biohybrids produced using CALB, analogous materials were synthesized using lipase from *Thermomyces lanuginosus* (TLL), which is an attractive option due to high thermal stability. Here, the attained silver and gold nanobiohybrids TLL/AgNP and TLL/AuNP both exhibited a slightly higher metal content of 33% and 19% (w/w) on ICP-OES analyses than the analogous CALB-hybrids (Table 1).

As mutual deactivation of the combined enzyme and metal entities through poisoning effects is a concern in the nanobiohybrid syntheses, we sought to combat this deactivation by implementing polymer additives in the structure of the enzyme-metal nanobiohybrids (Figure 3).<sup>[13]</sup> This is achieved by first producing protein bioconjugates, where ionic polymers are coated on the enzyme surface. The metal nanoparticles are then grown on the acquired bioconjugates.<sup>[14]</sup> A further range of biohybrids were produced, where polyethyleneimine (PEI) or modified dextran, which included a high number of aspartic acid groups (DexAsp), polymer chains were incorporated into the design. This approach proved successful, as using a CALB bioconjugated with smaller 6 kDa DexAsp polymer resulted in hybrid CALB/AgNP-2, where the metal nanoparticle size was more uniform than on the CALB/AgNP-1 (Figure 2). Using a much larger 2000 kDa DexAsp polymer for the bioconjugate production gave hybrid CALB/AgNP-3, where the incorporated polymer covers large areas of the protein aggregate surface, leading to the metal nanoparticles being slightly larger and less clustered (Figure 2). Similarly, hybrids CALB/AgNP-4 and CALB/AgNP-5 were synthesized using smaller 0.8 kDa and larger 750 kDa PEI polymers for the bioconjugation. The metal content in all of the produced bioconjugated CALB and Ag hybrids was similar to the CALB/AgNP-1, ranging from 21% to 26% (w/w) according to ICP-OES analyses (Table 1). Lastly, another gold nanobiohybrid was produced using the protein bioconjugates,

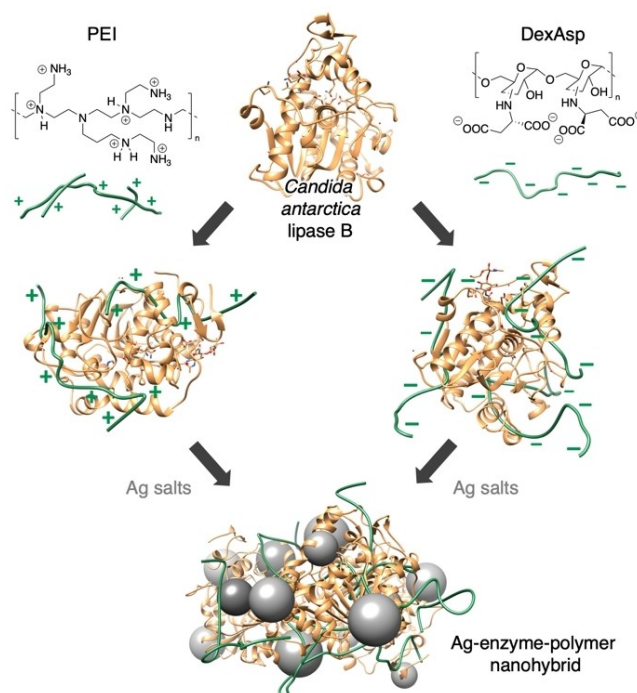


**Figure 3.** Synthesis of metal nanobiohybrids using enzyme-polymer conjugates.

as CALB conjugated with the 6 kDa DexAsp was used in the synthesis of hybrid CALB/AuNP-2. Here, the final Au content in the material was surprisingly low, at only 4% (w/w). Disappointingly, the polymer additives did not have the desired effect on the preservation of enzymatic activity, as the non-conjugated CALB/AgNP-1 remained the most active of the nanobiohybrids (Table S1). The metal activity was, however, improved by the inclusion of 6 kDa DexAsp on the bioconjugate CALB/AuNP-2,

which exhibited superior metal catalytic TOF compared to CALB/AuNP-1 (Table S2).

The synthesized nanobiohybrids were then evaluated for applicability for 2,5-dihydrofuran production from allenes. We screened the lipase-metal nanoparticle biohybrids for their ability to catalyze the cyclization of allenic alcohol **1a** (Table 2). Initial attempts to employ CALB/PdNP as the catalyst with tetrahydrofuran as the solvent resulted in a slow conversion, where 7% yield was achieved after 72 hours (Table 2, Entry 1), after 24 hours (Entry 2). The more environmentally friendly 2-methyltetrahydrofuran could also be used as the solvent for the catalysis, however the resulting yield of 78% was slightly diminished compared to tetrahydrofuran (Entry 3). Chosen reaction medium was found to have a strong effect on the performance of CALB/AuNP-1 hybrid, as using acetonitrile or *N,N*-dimethylformamide medium instead of tetrahydrofurans decelerated the reaction considerably, resulting in roughly 50% yields of the desired product after 72 hours (Entries 4 and 5), while non-polar *n*-heptane effectively shut down the reaction (Entry 6). The other tested nanobiohybrids besides CALB/AuNP-1 did not perform well in purely organic solvents, but were considerably aided by the presence of an aqueous component in the medium. Likely, the accessibility of the catalytic metal species is improved here by the added flexibility of the lipase material in the aqueous environment. In a 1:1 tetrahydrofuran-water mixture, CALB/AuNP-1's performance was hindered due to arising side reactions, resulting in 50% yield in 24 h (Entry 7). With this solvent system, the GOx/PdNP hybrid performed comparatively to the CALB/AuNP-1 (Entry 8). However, the Pd nanoparticles induced on the lipase support (CALB/PdNP) did not reach the same efficiency (Entry 9). In the tetrahydrofuran/water medium, CALB/AgNP-1 performed noticeably slower than the other tested biohybrids (Entry 10), exhibiting the difference in catalytic potential of silver for this transformation compared to related noble metals Pd and Au despite similar hybrid metal contents. Interestingly, using the polymer conjugated hybrid CALB/AuNP-2 the principal product was not the desired **3a**,

which was only obtained in minor amounts (Entry 11). In both entries 7 and 11 using the gold biohybrids in aqueous media, the arising product was identified as C–C coupled dimer of the 2,5-dihydrofuran **3a**. The same side product was also seen in the processes catalyzed by Pd-hybrids (Entries 7 and 8), with the hybrid CALB/PdNP producing more of the dimer than GOx/PdNP. The dimer is likely a result of further reactivity of the desired product **3a**, and the differences in the consumption of **3a** likely follows from the size distribution and accessibility of the metal nanoparticles in the heterogeneous hybrid materials. Similar dimerizations have been observed previously with stoichiometric gold-reagents or oxidant-dependent gold recycling processes.<sup>[15]</sup>

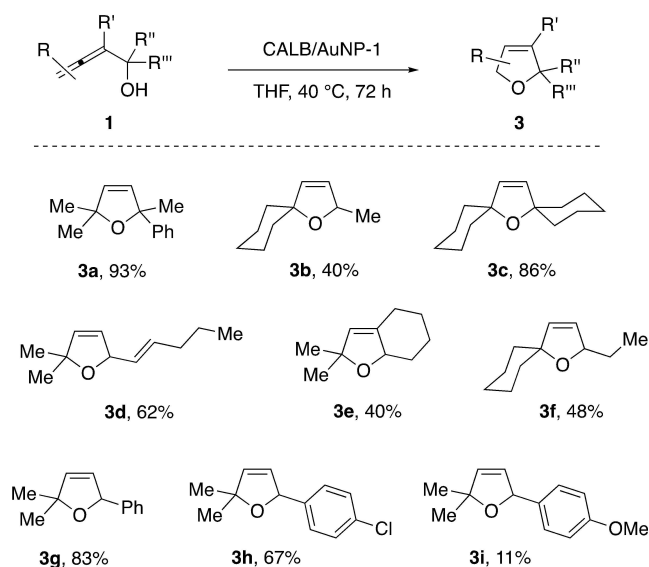
We subsequently evaluated the cyclization process on structurally varied  $\alpha$ -hydroxyallene analogues. Satisfyingly, the CALB/AuNP-1 was able to efficiently catalyze the formation of a range of 2,5-dihydrofurans **3** under the optimized conditions (Scheme 2). The two fully  $\alpha$ -substituted allenic alcohols **1a** and **1c** were cycloisomerized in very high ~90% yields, underlining the applicability of the heterogeneous catalysts for this type of processes. While  $\alpha$ -monosubstituted allenes were also cyclized in acceptable yields, they fell short of the efficiency achieved for the fully  $\alpha$ -substituted substrates. Including purely saturated hydrocarbons in the substitution pattern of the allene resulted in mediocre 40–50% conversions into the dihydrofurans **3b**, **3e** and **3f**, although the yields of these products may have been compromised in parts due to the volatility of the compounds. More activating substituents in an allylic olefin (**3d**) or aryl groups (**3g**, **3h**) generally improved the efficiency of the catalysis. However, the *p*-methoxyphenyl-substitution on the allenol  $\alpha$ -position decelerated the reaction significantly, resulting in recovery of the substrate after the 72 h reaction time with only 11% conversion to the desired dihydrofuran **3i**. The reason why this aromatic substitution slows the process so substantially could be in the added nucleophilicity of the aryl ring resulting in competing coordination to the gold-catalyst

**Table 2.** Enzyme-metal nanobiohybrids as catalysts for  $\alpha$ -hydroxyallene **1a** cycloisomerization.<sup>[a]</sup>

Entry	Biohybrid	Solvent	Time [h]	Yield [%]	Conversion [%]
1	CALB/PdNP	THF	72	7	17
2	CALB/AuNP-1	THF	24	90	> 99
3	CALB/AuNP-1	2-Me-THF	24	78	> 99
4	CALB/AuNP-1	MeCN	72	47	87
5	CALB/AuNP-1	DMF	72	49	77
6	CALB/AuNP-1	<i>n</i> -heptane	72	6	23
7	CALB/AuNP-1	THF/water 1:1	24	50	> 99
8	GOx/PdNP	THF/water 1:1	24	57	> 99
9	CALB/PdNP	THF/water 1:1	24	30	> 99
10	CALB/AgNP-1	THF/water 1:1	24	26	43
11	CALB/AuNP-2	THF/water 1:1	24	4	95

[a] Conditions: 9.4 mg (50  $\mu$ mol) allenol **1a**, 1.0 mg enzyme-metal biohybrid, 2 mL of indicated solvent system, 50 °C. Shaken at 800 rpm for indicated reaction time. Yields and conversions were determined by quantitative <sup>1</sup>H-NMR spectroscopy.





**Scheme 2.** Substrate scope of gold-nanoparticle biohybrid-catalyzed cyclizations of allenic alcohols **1**.

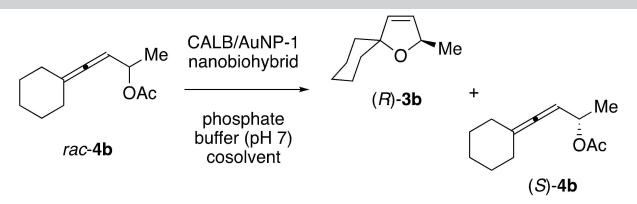
with the electron-rich arene instead of the allene  $\pi$ -orbitals, effectively suppressing the cyclization reactivity.

Having established the allenic alcohol cycloisomerization using the metal component of the nanobiohybrids, we attempted to combine the technique in cascade process with kinetic resolution hydrolysis catalyzed by the lipase-constituents of the hybrids. Racemic allenic acetate **4b** was selected as prototype substrate for the one-pot reaction development, while the screened hybrid was the one showing most promise in the allenol cyclizations, CALB/AuNP-1. Unfortunately, the initial attempts to implement a reaction medium with organic solvent as the major component resulted in complete inactivation of the CALB/AuNP-1 mediated transformation (Table 3,

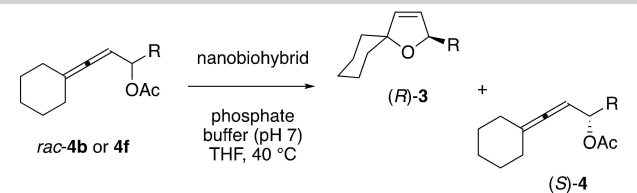
Entries 1 and 2). Reassuringly, moving to a more heavily aqueous solvent system at room temperature gave rise to production of desired (*R*)-**3b** in great selectivity of 93% *ee*, albeit with a slow conversion rate (Entry 3). Adopting the reaction medium used by Krause's group in their homogeneous catalysis improved the results further (Entries 4 and 5),<sup>[12a]</sup> where conversions of 17% and 21% were achieved after 24 and 48 h at 40 °C in 40:1 phosphate buffer (pH 7)/tetrahydrofuran mixture, respectively. While the kinetic resolution of the allenic acetate **4b** was not complete after 48 h (Entry 5), prolonged reaction time did not improve the results as side-reactions emerge to degrade the desired product similarly to already observed for the allenic alcohol cyclizations, leaving only 5% conversion to be recovered after a 96 hour reaction time (Entry 6). Omitting the organic component from the solvent system altogether (Entry 7) had minimal effect compared to the 40:1 buffer/tetrahydrofuran mixture. While there was no significant difference in the end result, the added practicality of delivering the substrate into the reaction vessel dissolved in the tetrahydrofuran component made us keep the organic portion in the medium moving forward.

We subsequently looked to evaluate all the synthesized lipase-metal nanoparticle biohybrids as catalysts for the hydrolytic cyclization design. Moving from gold to silver as the metal-component in the biohybrid resulted in slightly higher conversion of 26% after 96 hours, but diminished purity of 88% *ee* (Table 4, Entry 2), compared to the optimal 48 hour reaction time with CALB/AuNP-1 (Entry 1). Here, the product is not consumed in the undesired dimerization using the less reactive silver-species as the catalyst, allowing for higher conversions to be reached with prolonged reaction times. Strikingly, while palladium hybrid CALB/PdNP could be used in allenol cyclization to acceptable levels, it exhibited very low activity for the cascade process. Likely due to the metal constituent poisoning the needed enzyme catalyst, the reaction resulted in just 3% conversion after 72 h (Table 4, Entry 3). The nanobiohybrids

**Table 3.** Examining reaction conditions for CALB/AuNP-1 catalyzed hydrolysis/cyclization cascade of allenic acetate **4b**.

Entry <sup>[a]</sup>	Medium	T [°C]	Time [h]				
				(R)- <b>3b</b>		(S)- <b>4b</b>	
				[%]	<i>ee</i> [%]	[%]	<i>ee</i> [%]
1	buffer/THF (1:2)	40	48	–	–	100	0
2	buffer/acetone (1:2)	40	48	–	–	100	0
3	buffer/THF (10:1)	r.t.	48	7	93	82	21
4	buffer/THF (40:1)	40	24	17	90	70	40
5	buffer/THF (40:1)	40	48	21	93	60	64
6	buffer/THF (40:1)	40	96	5	87	51	93
7	buffer only	40	48	21	93	61	60

[a] Conditions: 19 mg (100  $\mu$ mol) allenic acetate **4b**, 3.0 mg CALB/AuNP-1 biohybrid, 2 mL phosphate buffer solution (0.1 M, pH 7) with co-solvent. Shaken at 800 rpm for indicated reaction time. Conversion and enantiomeric excess measured by chiral gas chromatography.

**Table 4.** Evaluation of lipase/metal nanobiohybrids in the hydrolytic cyclization cascade of allenic acetates.


Entry <sup>[a]</sup>	Lipase biohybrid	R	Time [h]	(R)-3		(S)-4	
				[%]	ee [%]	[%]	ee [%]
1	CALB/AuNP-1	Me	48	21	93	60	64
2	CALB/AgNP-1	Me	96	26	88	52	88
3	CALB/PdNP	Me	72	3	96	92	8
4	TLL/AuNP	Me	48	0	–	100	0
5	TLL/AgNP	Me	72	1	60	98	1
6	CALB/AuNP-2	Me	72	2	93	50	99
7	<b>CALB/AgNP-2</b>	Me	72	<b>43</b>	<b>94</b>	<b>50</b>	<b>94</b>
8	<b>CALB/AgNP-3</b>	Me	72	<b>42</b>	<b>95</b>	<b>53</b>	<b>84</b>
9	CALB/AgNP-4	Me	72	5	89	94	6
10	CALB/AgNP-5	Me	72	2	71	98	1
11	CALB/AgNP-3	Et	96	13	95	73	36

[a] 7.8 mg (40  $\mu$ mol) allenic acetate **4b** or **4f**, 1.5 mg lipase/MeNP biohybrid, 20  $\mu$ L tetrahydrofuran, 0.8 mL phosphate buffer solution (0.1 M, pH 7), 40 °C. Shaken at 800 rpm for indicated reaction time. Conversion and enantiomeric excess measured by chiral gas chromatography.

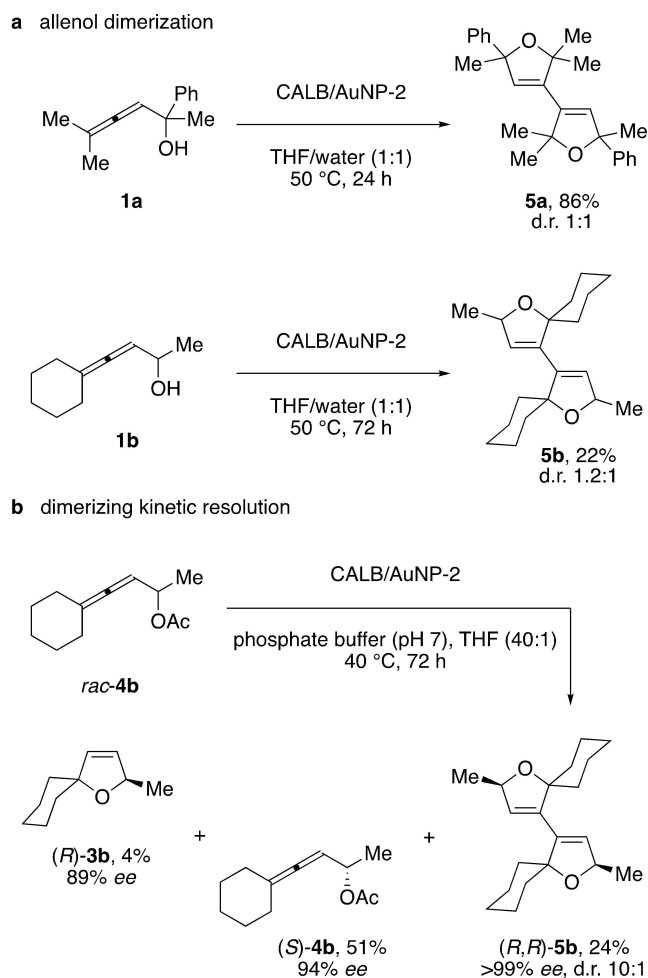
incorporating TLL as the protein support for the formation of metal nanoparticles were also tested for the one-pot design. However, both TLL/AuNP and TLL/AgNP failed to reach notable conversions within reasonable time (Table 4, Entries 4 and 5). Next, we tested the nanobiohybrids, where the various polymer additives had been used for bioconjugation. CALB/AuNP-2, where 6 kDa DexAsp was incorporated to the synthesis, was very effective for purifying the unreactive (S)-**4b** enantiomer, reaching 99% ee for the substrate (Entry 6). However, the conversion into the desired product (R)-**3b** was negligible, due to similar side-reactions as observed for cyclizations of **1a** using the Au biohybrids during the slow release of allenols by the lipase. On the contrary, incorporating DexAsp as additive in the synthesis of the silver-nanoparticle biohybrids CALB/AgNP-2 (6 kDa) and CALB/AgNP-3 (2 MDa) resulted in highly effective heterogeneous catalysts for this cascade process, as great conversions of 42–43% were achieved employing them, while purity of the product (R)-**3b** was also on desirable level at 94–95% ee (Table 4, Entries 7 and 8). Compared to the slower rate of catalysis with the non-conjugated CALB/AgNP-1, the polymer-conjugation likely facilitates the rate increase by allowing more separation within the structure of the nanomaterial, resulting in better accessibility of the catalytic species (Figure 2). Inclusion of polyethyleneimine bioconjugates in the silver nanobiohybrid formation failed to produce as effective catalysts for this transformation as the inclusion of DexAsp, as CALB/AgNP-4 and CALB/AgNP-5 were able to catalyze only minor conversions into (R)-**3n** (Table 4, Entries 9 and 10). The extension of the protocol is mainly defined by the acceptance and selectivity of the lipase matrix following the common trends in sterics vs activity/selectivity. Hence, while the slightly larger ethyl-substituted allenic acetate **4f** showed substantially reduced turnover by the CALB-based biohybrid, the dihydrofuran (R)-**3f** was still produced in excellent stereoselectivity with 95%

ee (Table 4, Entry 11) whereas a prolonged reaction time would be required to achieve satisfactory conversions.

Finally, we took a closer look at the dimerization event leading to symmetrically fused dihydrofuran products that were observed during the initial method development. While the dimers **5** were obtained in processes using all of the different Au and Ag nanobiohybrids as catalysts, the most effective hybrid for this transformation was identified to be the DexAsp-conjugated CALB/AuNP-2. Strikingly, the allenic alcohol **1a** could be transformed this way almost quantitatively into the bis-dihydrofuran **5a** (Scheme 3). As previously reported methods for this type of oxidative C–C coupling by gold complexes have so far been dependent of harsh oxidizers such as Selectfluor,<sup>[15]</sup> future research will aim at investigating this curious behavior of some selected nanobiohybrids that enables them to catalyze the reaction under mild aerobic conditions. Utilizing the same CALB/AuNP-2, the less densely substituted allenol **1b** was also transformed into the corresponding tetracyclic **5b** in reasonable 22% yield. Encouraged by this, we attempted to use the newly found protocol for stereoselective production of the interesting multi-cyclic structure. Using racemic allenic acetate **4b** as the substrate, the bis-dihydrofuran (R,R)-**5b** was reached in great enantio- and diastereoselectivity with a yield of 24%. The results illustrate the flexibility and usefulness of the enzyme-metal nanoparticle biohybrid approach, as with careful tuning of the constituents the reactivity of the protocol can be shifted from producing the monomeric dihydrofuran **3b** to the dimeric **5b** both with excellent yield and stereopurity.

## Conclusion

Lipase/metal nanoparticle biohybrids proved excellent heterogeneous catalysts for stereoselective hydrolytic cyclization of



**Scheme 3.** Aerobic dimerization of allenes to 3,3'-bis-dihydrofurans (dimer yields correspond to the reaction stoichiometry, i.e. 2 moles of allene can form a maximum of 1 mole of the dimer).

allenic acetate **4b** to furnish 2,5-dihydrofuran (*R*)-**3b** through a kinetic resolution cascade process. Incorporating novel enzyme-polymer bioconjugates into the nanobiohybrid syntheses gave access to robust dual-active entities capable of mediating both reaction steps in the one-pot design. The hybrids combining silver nanoparticles with DexAsp-conjugated CALB enzyme were found most effective for the process, giving over 40% conversions and 95% optical purity for the desired *O*-heterocycle. Wider applicability of the biohybrid approach was tested on the metal-catalyzed allenol cycloisomerizations. Here, a variety of 2,5-dihydrofurans were efficiently produced from  $\alpha$ -hydroxyallenes using a biohybrid consisting of CALB and gold nanoparticles, with more densely substituted allenes giving higher yields in the process. The results exemplify the nanobiohybrid approach's great potential for heterogeneous multi-activity catalysis in novel tailor-made one-pot reaction schemes.

## Experimental Section

### General remarks

All reactions carried out in dry solvents were performed under argon atmosphere using anhydrous conditions. Anhydrous solvents were acquired from an MBraun MB-SPS800 drying system. Commercially available reagents were used without further purification unless otherwise noted. Enzymes were obtained from: *Candida antarctica* lipase B (CALB), Novozymes; *Thermomyces lanuginosus* lipase (TLL), Novozymes; glucose oxidase from *Aspergillus niger* (GOx), Novozymes. Nanobiohybrids were prepared according to a previously reported protocol.<sup>[14]</sup> Synthesized products were purified by column chromatography over silica gel (Macherey-Nagel MN-Kieselgel 60, 40–60  $\mu$ m, 240–400 mesh) or by distillation. Reactions were monitored by thin layer chromatography (TLC) carried out on pre-coated silica gel plates (Merck, TLC Silica gel 60 F254) using UV light and  $\text{KMnO}_4$ -solution for visualization. NMR, IR, GC, optical rotation and HRMS data of the synthesized compounds were recorded at the Department of Chemistry of Aalto University.  $^1\text{H}$  and  $^{13}\text{C}$ -NMR spectra were recorded with a Bruker Avance NEO 400 ( $^1\text{H}$  400.13 MHz,  $^{13}\text{C}$  100.62 MHz). The chemical shifts are reported in parts per million (ppm) in relation to non-deuterated chloroform signal ( $^1\text{H}$ -NMR:  $\delta = 7.26$ ;  $^{13}\text{C}$ -NMR:  $\delta = 77.16$ ). Quantitative  $^1\text{H}$ -NMR were recorded using delay time  $D = 30$  s and  $30^\circ$  pulse, and are reported in relation to dimethyl sulfone internal standard signal ( $\delta = 3.00$ , s, 6 H). Infrared spectra were recorded at room temperature on a Bruker Alpha ECO-ATR FT-IR-Spectrometer, absorption bands are reported in wave numbers [ $\text{cm}^{-1}$ ]. Optical rotations were measured using an Autopol VI Automatic Polarimeter from Rudolph Research Analytical or a DIP-1000 Digital Polarimeter from Jasco. Gas chromatography was performed on a Shimadzu GC-2010 Plus gas chromatograph using a Supelco Analytical Beta DEX 120 column (30 m  $\times$  0.25 mm), with column flow 2.55  $\text{mL min}^{-1}$  and temperature program: 50  $^\circ\text{C}$  (2 min)/20  $^\circ\text{C min}^{-1}$ /115  $^\circ\text{C}$  (35 min). High resolution mass spectrometry was performed on an Agilent 6530 (Q-TOF) mass spectrometer or a Bruker MicroTOF mass spectrometer. Enzyme-metal hybrids were analyzed by ICP-OES, XRD, TEM and SEM at the Institute of Catalysis (ICP-CSIC). Inductively coupled plasma optical emission spectroscopy (ICP-OES) was performed on a Perkin Elmer OPTIMA 2100 DV equipment. Transmission electron microscopy (TEM) was done using a JEOL JEM-2100F field emission electron microscope equipped with an EDX detector INCA x-sight (Oxford Instruments). Scanning electron microscopy (SEM) was performed using a Hitachi TM-1000 tabletop microscope. Lyophilization of the hybrids was done using a Telstar LyoQuest laboratory freeze-dryer.

### Synthesis of racemic 2,5-dihydrofurans

A vial was charged with allenic alcohol **1a–1i** (100  $\mu$ mol) in tetrahydrofuran (2 mL). CALB/AuNP-1 biohybrid (3.0 mg) was added, and the suspension was shaken on 800 rpm at 40  $^\circ\text{C}$  for 3 days. Solid materials were removed from the reaction mixture by filtration, and the filtrate was concentrated under reduced pressure. Purification of the crude products by flash chromatography ( $\text{SiO}_2$ , *n*-pentane/diethyl ether 50:1) gave the expected 2,5-dihydrofurans **3a–3i** (Scheme 2).

### Representative procedure for stereoselective 2,5-dihydrofuran synthesis

Into a vial charged with 0.8 mL aqueous phosphate buffer solution (0.1 M, pH 7) was added allenic acetate *rac*-**4b** (7.8 mg, 40  $\mu$ mol) in 20  $\mu$ L tetrahydrofuran. CALB/AgNP-2 biohybrid (1.5 mg) was added

to the vial, and the suspension was shaken on 800 rpm at 40 °C for 3 days. After, the mixture was extracted with ethyl acetate (4 × 1 mL). Solid materials were removed from the combined organic layers by filtration. The solution was analyzed by GC, revealing a 43% conversion into 2,5-dihydrofuran (*R*)-**3b** (94% *ee*). After removal of solvents under reduced pressure, crude products were purified by flash chromatography (SiO<sub>2</sub>, *n*-pentane/diethyl ether 25:1) to give the expected products (*R*)-**3b** and (*S*)-**4b** (Table 4).

## Acknowledgements

We gratefully acknowledge financial support by the European Research Council (ABLONYS, 865885), the Academy of Finland (grant numbers 298250 and 324976), the COST action CA15106 (CHAOS), the Ruth & Nils-Erik Stenbäck's Stiftelse, and the Finnish Cultural Foundation. The authors thank the support by the Spanish National Research Council (CSIC) and the Portuguese Research Foundation (EXPL/QUI-QOR/1079/2021).

## Conflict of Interest

The authors declare no conflict of interest.

## Data Availability Statement

The data that support the findings of this study are available in the supplementary material of this article.

**Keywords:** nanoparticles · lipases · cascades · heterocycles · dual catalysis

- [1] Y. Hayashi, *Chem. Sci.* **2016**, *7*, 866–880.
- [2] a) R. A. Sheldon, J. M. Woodley, *Chem. Rev.* **2018**, *118*, 801–838; b) J. Nazor, J. Liu, G. Huisman, *Curr. Opin. Biotechnol.* **2021**, *69*, 182–190; c) M. A. Huffman, A. Fryszkowska, O. Alvizo, M. Borra-Garske, K. R. Campos, et al., *Science* **2019**, *366*, 1255–1259; d) Y.-C. Liu, C. Merten, J. Deska, *Angew. Chem. Int. Ed.* **2018**, *57*, 12151–12156; *Angew. Chem.* **2018**, *130*, 12328–12333.
- [3] a) Y. Liu, P. Liu, S. Gao, Z. Wang, P. Luan, J. González-Sabín, Y. Jiang, *Chem. Eng. J.* **2021**, *420*, 127659; b) F. Rudroff, M. D. Mihovilovic, H. Gröger, R. Snajdrova, H. Iding, U. T. Bornscheuer, *Nat. Catal.* **2018**, *1*, 12–22; c) S. Schmidt, K. Castiglione, R. Kourist, *Chem. Eur. J.* **2018**, *24*, 1755–1768; d) O. Verho, J.-E. Bäckvall, *J. Am. Chem. Soc.* **2015**, *137*, 3996–4009; e) L. E. Heim, D. Thiel, C. Gedig, J. Deska, M. H. G. Precht, *Angew. Chem. Int. Ed.* **2015**, *54*, 10308–10312; *Angew. Chem.* **2015**, *127*, 10447–10451; f) G. Tavakoli, J. E. Armstrong, J. M. Naapuri, J. Deska, M. H. G. Precht, *Chem. Eur. J.* **2019**, *25*, 6474–6481.
- [4] a) J. M. Palomo, *Chem. Commun.* **2019**, *55*, 9583–9589; b) M. Filice, M. Marciello, M. del Puerto Morales, J. M. Palomo, *Chem. Commun.* **2013**, *49*, 6876–6878; c) T. Cuenca, M. Filice, J. M. Palomo, *Enzyme Microb. Technol.* **2016**, *95*, 242–247.
- [5] a) R. Bussamara, D. Eberhardt, A. F. Feil, P. Migiowski, H. Wender, D. P. de Moraes, G. Machado, R. M. Papaléo, S. R. Teixeira, J. Dupont, *Chem. Commun.* **2013**, *49*, 1273–1275; b) A. C. Franzoi, I. Cruz Vieira, C. Weber Scheeren, J. Dupont, *Electroanalysis* **2010**, *22*, 1376–1385; c) H. Konnerth, M. H. G. Precht, *Green Chem.* **2017**, *9*, 2762–2767; d) A. Weillhard, G. A. Abarca, J. Viscardi, M. H. G. Precht, J. D. Scholten, F. Bernardi, D. L. Baptista, J. Dupont, *ChemCatChem* **2017**, *9*, 204 211; e) H. Konnerth, M. H. G. Precht, *Chem. Commun.* **2016**, *52*, 9129–9132; f) M. T. Keßler, S. Robke, S. Sahler, M. H. G. Precht, *Catal. Sci. Technol.* **2014**, *4*, 102–108.
- [6] a) S. Yu, S. Ma, *Angew. Chem. Int. Ed.* **2012**, *51*, 3074–3112; *Angew. Chem.* **2012**, *124*, 3128–3167; b) N. Krause, A. S. K. Hashmi, *Modern allene chemistry*, Wiley-VCH, Weinheim, **2004**.
- [7] a) N. Krause, C. Winter, *Chem. Rev.* **2011**, *111*, 1994–2009; b) J. M. Alonso, P. Almendros, *Chem. Rev.* **2021**, *121*, 4193–4252; c) J. Naapuri, J. D. Rolfes, J. Keil, C. Manzuna Sapu, J. Deska, *Green Chem.* **2017**, *19*, 447–452; d) J. Deska, J.-E. Bäckvall, *Org. Biomol. Chem.* **2009**, *7*, 3379–3381; e) N. Morita, N. Krause, *Org. Lett.* **2004**, *6* (22), 4121–4123.
- [8] J. M. Naapuri, G. A. Åberg, J. M. Palomo, J. Deska, *ChemCatChem* **2021**, *13*, 763–769.
- [9] a) Y. Wang, K. Zheng, R. Hong, *J. Am. Chem. Soc.* **2012**, *134*, 4096–4099; b) B. Gockel, N. Krause, *Eur. J. Org. Chem.* **2010**, 311–316; c) C. Manzuna Sapu, J.-E. Bäckvall, J. Deska, *Angew. Chem. Int. Ed.* **2011**, *50*, 9731–9734; *Angew. Chem.* **2011**, *123*, 9905–9908; d) C. Manzuna Sapu, J. Deska, *Org. Biomol. Chem.* **2013**, *11*, 1376–1382.
- [10] B. Alcaide, P. Almendros, A. M. González, A. Luna, S. Martínez-Ramírez, *Adv. Synth. Catal.* **2016**, *358*, 2000–2006.
- [11] a) Z. S. Seddigi, M. S. Malik, S. A. Ahmed, A. O. Babalghith, A. Kamal, *Coord. Chem. Rev.* **2017**, *348*, 54–70; b) A. Patti, C. Sanfilippo, *Symmetry* **2020**, *12*, 1454; c) C. Manzuna Sapu, T. Görbe, R. Lihammar, J.-E. Bäckvall, J. Deska, *Org. Lett.* **2014**, *16* (22), 5952–5955; d) B. Skrobo, J. Deska, *Org. Lett.* **2013**, *15* (23), 5998–6001.
- [12] a) M. Asikainen, N. Krause, *Adv. Synth. Catal.* **2009**, *351*, 2305–2309; b) B. Yang, C. Zhu, Y. Qiu, J.-E. Bäckvall, *Angew. Chem. Int. Ed.* **2016**, *55*, 5568–5572; *Angew. Chem.* **2016**, *128*, 5658–5662.
- [13] a) J. M. Bolivar, J. Rocha-Martin, C. Mateo, F. Cava, J. Berenguer, R. Fernandez-Lafuente, J. M. Guisan, *Biomacromolecules* **2009**, *10*, 742–747; b) O. Romero, C. W. Rivero, J. M. Guisan, J. M. Palomo, *PeerJ* **2013**, *1*, e27; c) C. A. Godoy, B. de las Rivas, M. Filice, G. Fernández-Lorente, J. M. Guisan, J. M. Palomo, *Process Biochem.* **2010**, *45*, 534–541; d) X. Li, Y. Cao, K. Luo, Y. Sun, J. Xiong, L. Wang, Z. Liu, J. Ma, J. Ge, H. Xiao, R. N. Zare, *Nat. Catal.* **2019**, *2*, 718–725; e) M. van der Verren, V. Smeets, A. vander Straeten, C. Dupont-Gillain, D. P. Debecker, *Nanoscale Adv.* **2021**, *13*, 1646–1655.
- [14] J. M. Naapuri, N. Losada García, J. Deska, J. M. Palomo, *Nanoscale* **2022**, *14*, 5701–5715.
- [15] a) R. Zhang, Q. Xu, K. Chen, P. Gu, M. Shi, *Eur. J. Org. Chem.* **2013**, 7366–7371; b) A. S. K. Hashmi, M. C. Blanco, D. Fischer, J. W. Bats, *Eur. J. Org. Chem.* **2006**, 1387–1389.

Manuscript received: March 14, 2022  
Revised manuscript received: April 20, 2022  
Accepted manuscript online: May 11, 2022  
Version of record online: June 22, 2022